Osteoarthritis and Cartilage 27 (2019) 810–822

Osteoarthritis and Cartilage

# The evolving large-strain shear responses of progressively osteoarthritic human cartilage

F. Maier †, C.G. Lewis ‡, D.M. Pierce † § *

† University of Connecticut, Department of Mechanical Engineering, Storrs, CT, USA
‡ Hartford Healthcare, Bone & Joint Institute, Hartford, CT, USA
§ University of Connecticut, Department of Biomedical Engineering, Storrs, CT, USA

ARTICLE INFO

*Article history:*
Received 7 September 2018
Accepted 28 December 2018

*Keywords:*
Human articular cartilage
Early-stage osteoarthritis
Large-strain shear
Energy dissipation
Stress
Strain

SUMMARY

*Objective:* The composition and structure of articular cartilage evolves during the development and progression of osteoarthritis (OA) resulting in changing mechanical responses. We aimed to assess the evolution of the intrinsic, large-strain mechanics of human articular cartilage—governed by collagen and proteoglycan and their interactions—during the progression of OA.
*Design:* We completed quasi-static, large-strain shear tests on 64 specimens from ten donors undergoing total knee arthroplasty (TKA), and quantified the corresponding state of OA (OARSI grade), structural integrity (PLM score), and composition (glycosaminoglycan and collagen content).
*Results:* We observed nonlinear stress–strain relationships with distinct hystereses for all magnitudes of applied strain where stiffnesses, nonlinearities, and hystereses all reduced as OA advanced. We found a reduction in energy dissipation density up to 80% in severely degenerated (OARSI grade 4, OA-4) vs normal (OA-1) cartilage, and more importantly, we found that even cartilage with a normal appearance in structure and composition (OA-1) dissipated 50% less energy than healthy (control) load-bearing cartilage ($HL_0$). Changes in stresses and stiffnesses were in general less pronounced and did not allow us to distinguish between healthy load-bearing controls and very early-stage OA (OA-1), or to distinguish consistently among different levels of degeneration, i.e., OARSI grades.
*Conclusions:* Our results suggest that reductions in energy dissipation density can be detected by bulk-tissue testing, and that these reductions precede visible signs of degeneration. We highlight the potential of energy dissipation, as opposed to stress- or stiffness-based measures, as a marker to diagnose early-stage OA.


## Introduction

Osteoarthritis (OA) initiates with deaggregation of glycosaminoglycans (GAGs), increased osmotic pressure[1], and softening of the collagen network[2]. Subsequently, chondrocytes "activate" and increase production of both matrix proteins and matrix degrading enzymes[3,4]. The permeability of cartilage also increases in OA, subsequently reducing the tissue's ability to generate and maintain hydrostatic pressure under load[5,6]. Furthermore, OA cartilage presents changes in zonal thicknesses and fiber orientations visible with both polarized light microscopy[7] and small angle X-ray scattering[8]. These changes in the mechanics of the tissue eventually exacerbate initial SZ collagen fibrillation into surface fissures, matrix loss, and erosion[9].

Such changes to the tissue's composition and structure also lead to altered mechanical responses typical of OA. Franz *et al.*[10] and Garcia-Seco *et al.*[11] showed changes in both structural integrity and composition correlated (respectively) with cartilage softening measured by indentation. Similarly, Robinson *et al.*[12] demonstrated that cartilage under large strain compression (up to 30%) softens with the onset of OA. These studies used loading rates resembling those *in vivo*, where poroelastic effects (i.e., pressure in the interstitial fluid) dominate the mechanical responses, and did not investigate the decoupled mechanical response of the solid constituents.

Any mechanical changes in cartilage might be exploited as biomechanical markers for detection of OA. For human OA cartilage,

* Address correspondence and reprint requests to: D.M. Pierce, University of Connecticut, Department of Mechanical Engineering, Storrs, CT, USA.
*E-mail address:* dmpierce@engr.uconn.edu (D.M. Pierce).

https://doi.org/10.1016/j.joca.2018.12.025
1063-4584/

Kleemann *et al.*[13] showed the equilibrium modulus, measured in unconfined compression, reduced with increasing degeneration, a significant difference for severe late-stage OA vs healthy control tissue, but not for mild OA (ICRS grade 1) vs healthy control (ICRS grade 0). Similarly, Kumar *et al.*[14] showed the parameters resulting from a time-dependent viscoelastic model fitted to indentation tests on progressively osteoarthritic cartilage correlated with degeneration, but also could not resolve the early stages of OA. In both studies the use of ICRS grading to quantify the progression of OA may have contributed to lack of sensitivity in detecting early-stage OA. ICRS grading focuses on macroscopic appearance and may not adequately capture pathological changes relevant to changes in mechanical properties, e.g., PG depletion. Use of alternative methods to quantify the progression of OA, especially those designed to distinguish among early stages of OA, i.e., the OARSI grading method[15], could aid in better understanding of initiation of OA.

Chan *et al.*[16] experimentally demonstrated that shear strains (approaching 12%) generally exceeded compressive strains under *in vivo* compression, highlighting the need to understand cartilage mechanics in large-strain shear; however, few studies have investigated degraded or diseased cartilage under shear. Only Wong *et al.*[17] tested human OA cartilage under large-strain shear and reported increased strains near the articular surface. This study focused on the frictional properties of OA cartilage and restricted the articular surface using only friction of the opposing surface, making the applied deformation difficult to control and perhaps affecting the measured bulk shear properties.

There is a clear need to investigate the evolution of large-strain cartilage mechanics associated with early-stage OA to 1) better understand disease initiation and progression (to identify possible treatment targets), 2) identify potential biomarkers for OA diagnosis (to test therapeutics), and 3) calibrate and validate advanced constitutive models (to better predict the initiation and progression of OA[18]).

In this study we quantify the evolution of the intrinsic, large-strain mechanics of the solid constituents of human articular cartilage, i.e., collagen and proteoglycan and their interactions[19,20], during the progression of OA as determined by OARSI grading. We correlate the evolution of measured bulk mechanical properties with measures of disease progression, structural integrity, and cartilage composition, and compare against results from healthy control cartilage (previously published in Maier *et al.*[21]) for context.

## Materials and methods

Using a triaxial shear testing device (Messphysik, Fuerstenfeld, AT) we completed displacement-driven, large-strain tests on 64 specimens of progressively osteoarthritic human articular cartilage (following Maier *et al.*[21]) as determined by both the OARSI grade and the PLM-CO score (cf. Table AIII).

### *Preparation of specimens*

We harvested ten lateral femoral condyles (three male and seven female, aged 65.8±12.5 years) from patients undergoing total knee arthroplasty (TKA) at Hartford Healthcare Bone & Joint Institute. We kept the condyles submerged in PBS at 4°C until we prepared specimens in our lab (within 8 h of extraction); thereafter we stored the specimens submerged in PBS at − 80°C until mechanical testing.

We first determined the split-line direction (SLD, Below et al.[22]) by pricking the articular surface with a needle dipped in India ink. We then extracted pairs of specimens from various load-bearing regions[23,21] locations across the donor joint − one for histological assessment (Section Histological assessment) and quantification of constituents (Section Quantification of constituents) and the second, directly adjacent, for mechanical testing (cubiod, $3 \times 3$ mm$^2$ footprint, full thickness and with one edge aligned parallel to the local SLD if distinctly present; Section Triaxial shear test). For specimens dedicated to mechanical testing we carefully removed the underlying trabecular bone and sufficient subchondral bone both to create a surface parallel to the articular surface and to ensure the intact cartilage–bone interface mimicked the *in situ* boundary conditions while testing[24]. We fixed the specimens for histological assessment in 10% neutral buffered formalin.

### *Histological assessment*

After decalcification in 0.5 M EDTA for 1 week, we embedded the specimen in paraffin and sectioned at 6 $\mu$m. To quantify overall cartilage health, we stained slides with Safranin-O fast green (Novaultra Safranin O stain kit, IHC World, Ellicott City, MD) and then applied the OARSI grading method[15]. Two independent, trained observers (FM, DP) determined the local OARSI grade, and we considered specimens ranging from OARSI grade 1 (normal) to 4.5 (severe disease) for mechanical testing. We binned the specimens into four groups based on their OARSI grade: normal (OA-1, grade $<$ 2), mild (OA-2, 2 $\leq$ grade $<$ 3), moderate (OA-3, 3 $\leq$ grade $<$ 4), and severe (OA-4, grade $\geq$ 4) OA.

To assess the integrity of the zonal architecture, i.e., heterogeneity in the network of collagen fibers, we stained additional slides with PicroSirius red (Novaultra Sirius red stain kit, IHC World) and examined these under polarized light. Two independent, trained observers (FM, LM) quantified the zonal architecture using the PLM-CO score[25]. This score uses an ordinal scale, ranging from disorganized (score 0) to that resembling a healthy control zonal architecture (score 5). We binned the specimens into two groups based on their PLM-CO score: specimens with evident zones (EZ, PLM-CO $>$ 3) and specimens without (NZ, PLM-CO $<$ 3).

If necessary to image an entire specimen, we acquired multiple images and stitched them together using the MosaicJ plugin for ImageJ (1.51n, National Institutes of Health, Bethesda, MD).

### *Quantification of constituents*

To quantify the mass fractions of the constituents, we sectioned cartilage specimens fixed for long-term storage, and we then deparaffinized and dried the specimens, removed any subchondral bone, and measured their dry weights. We then rehydrated the specimens with a decreasing alcohol series to PBS[26], and measured the wet weight. We completed digestion and analyses using a Glycosaminoglycan Assay Kit (6022, Chondrex, Redmond, WA) and a Hydroxyproline Assay Kit (6017, Chondrex). For analyses we used approximately 10 mg of tissue, solubilized in 1.25 ml digestive solution (125 $\mu$g/ml Papain (60,224, Chondrex) in PBS at pH 6.3 with 5 mM L-cystein-HCL and 10 mM EDTA-2Na), incubated at 65°C for 36 h. We then centrifuged this solution at 10,000 rpm for 5 min and transferred the supernatant for analyses with the GAG assay. After determining the GAG concentration, we hydrolyzed 100 $\mu$l of the dissolved tissue in 10 N hydrochloric acid and quantified hydroxyproline concentration. We multiplied this concentration by

7.4 to get total collagen (following the protocol from Chondrex). We reported all concentrations per wet and dry weight.

### *Triaxial shear test*

We used our testing device and protocol as previously described in Maier *et al.*[21]. Briefly, we performed quasi-static (75 $\mu$m/min) cyclic simple shear tests, both parallel and perpendicular to the local SLD (when present), on cartilage specimens under 1% precompression. To improve adherence, we glued specimens to polymethyl methacrylate (PMMA) platens which we glued to stainless steel platens using cyanoacrylate gel. At each phase of the test we allowed specimens to equilibrate, i.e., after gluing, after applying precompression, and when changing the loading direction for 2,000, 4,000, and 600 s respectively. We applied maximum displacements corresponding to shear strains of ±5%, ±10%, ±15%, and ±20% (with respect to the undeformed thickness) for six cycles per direction and measured the corresponding reaction forces in time. We completed all tests in a bath of PBS at 37±1°C including antibiotics (100 U/ml penicillin and 100 mg/ml streptomycin) and protease inhibitors (Sigma Aldrich, St. Louis, MO) to avoid tissue degeneration.

### *Data analyses*

We calculated the shear strain $\gamma$ and corresponding shear stress $\tau$ as

$$\gamma = \frac{\Delta l}{L} \quad \text{and} \quad \tau = \frac{f}{A}, \tag{1}$$

where $\Delta l$ is the applied displacement, $L$ is the undeformed thickness of the specimen, $f$ is the measured force, and $A$ is the cross-section (footprint) of the specimen parallel to the measured force. For subsequent analyses we calculated the strain-energy dissipation density ($E_{DI}$) and the peak-to-peak shear stress ($\tau_{PP}$) at each applied strain magnitude as

$$E_{DI} = \oint_{\gamma_{min}}^{\gamma_{max}} \tau d\gamma, \tag{2}$$

and

$$\tau_{PP} = \tau(\gamma_{max}) - \tau(\gamma_{min}), \tag{3}$$

where $\gamma_{max}$ and $\gamma_{min}$ are the maximum and minimum shear strain of a given loading cycle. We also calculated the peak effective shear modulus ($G_{PE}$) by progressively finding the slopes of linear least-squares fits over ten progressive data points along our stress–strain loading curves[27]. For each applied strain magnitude, we determined both the positive and negative slopes as

$$G^{+/-} = \frac{\tau_{ave}}{\gamma_{ave}}, \quad \text{where} \begin{cases} \text{for } +, & \tau_{ave} \geq 0 \text{ and } \gamma_{ave} \geq 0 \\ \text{for } -, & \tau_{ave} < 0 \text{ and } \gamma_{ave} < 0 \end{cases}, \tag{4}$$

for all linear fits along each loading curve, and where $\tau_{ave}$ is the vertical projection of the best-fit line and $\gamma_{ave}$ is the complementary horizontal projection. After determining the maximum positive and negative slopes, $G^{+}_{max}$ and $G^{-}_{max}$, we averaged them to obtain the peak effective shear modulus $G_{PE}$ at each strain magnitude. Figure 1 illustrates our mechanical data analyses. In our tests the force responses were repeatable after three preconditioning cycles, and we averaged all calculated values over the next three loading cycles.

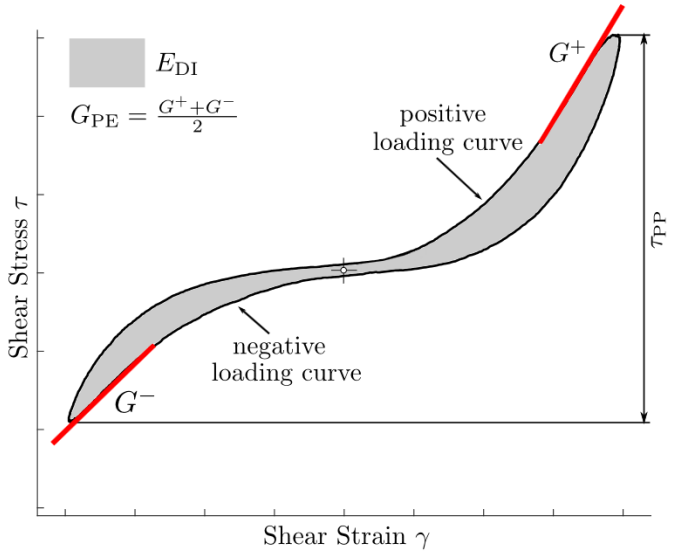


**Fig. 1.** Schematic visualization of energy-dissipation density ($E_{DI}$), peak-to-peak shear stress ($\tau_{PP}$), and peak effective shear modulus ($G_{PE}$) applied to our shear testing data.

We completed all calculations using MATLAB R2017a (The MathWorks Inc., Natick, MA), cf[21].

### *Statistical analyses*

We determined the minimum number of specimens for each OA group ($n = 5$) using a power analysis based on our data from a preliminary experiment. This minimum number provides a power of 84.6% for predicting a 50 kPa change in peak-to-peak shear stresses with an estimated standard deviation of 20 kPa and with a 95% level of significance.

First, using a Shapiro–Wilk test, we confirmed that the outputs of our mechanical data analyses were normally distributed. To validate inter-observer agreement in our application of the OARSI and PLM-CO grading methods we calculated the linear weighted Cohen's kappa coefficient $\kappa$. Furthermore, we used an ordinal regression to see how OA (OARSI grade) affects structure (PLM score). To probe for anisotropy, we used the Wilcoxon Rank–Sum test to compare mechanical responses parallel and perpendicular to the local SLD. To probe for effects from progressing OA, we conducted Kruskal–Wallis tests on composition (proteoglycan and collagen content), structure (PLM-CO score, thickness), and mechanics ($E_{DI}$, $\tau_{PP}$, $G_{PE}$) of cartilage gathered from OA knees (OA-1 to -4).

To further assess influence of OA, we used data from young, healthy control cartilage (30.2 ± 8.8 years), published in our previous work[21], as a benchmark. Data on healthy control cartilage corresponds to load-bearing at 0° knee flexion ($HL_0$, $n = 6$) and non-load bearing, i.e., covered by the menisci, (HNL, $n = 6$) regions. These data represent upper and lower bounds on healthy cartilage, as they are the stiffest and softest healthy adult cartilage from the lateral condyles.

When we identified significant correlations, we used pairwise comparisons (two-tailed Student's $t$-test or Wilcoxon Rank–Sum test, depending on normality) to identify significant differences within OA groups (number of comparisons $m = 6$) and to compare OA groups to healthy controls ($m = 4$). We assessed the influence of

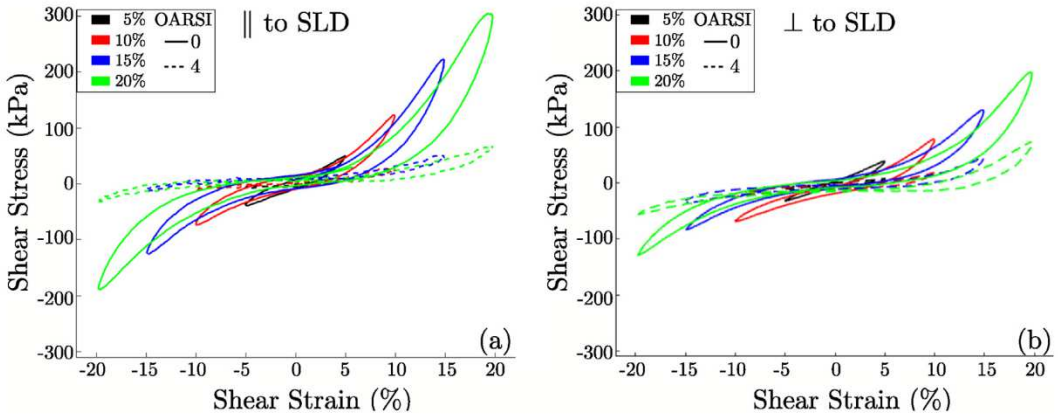


**Fig. 2.** Representative shear stress–strain plots of normal (OARSI grade 1) and severely degenerated (OARSI grade 4) specimens (a) parallel and (b) perpendicular to the local split-line direction.

proteoglycan and collagen content, age, and thickness on our mechanical metrics using Pearson's (Spearman's) correlation coefficient $r$ ($r_S$) ($m = 4$). We used $\alpha = 0.05$ to test for significance and adjusted this for our multiple comparison tests using the Holm-Bonferroni method ($\alpha = 0.05/m$).

We completed all statistical analyses using SAS 9.4 (SAS Institute Inc., Cary, NC).

## Results

We completed a total of 512 shear tests using 64 specimens. We show representative shear stress–strain plots comparing specimens with OARSI grade 0 and OARSI grade 4 in Fig. 2. We observed nonlinear stress–strain relationships with distinct hystereses for all magnitudes of applied strain where stiffness, nonlinearity, and hysteresis reduce with advancing OA.

Thirty of our cartilage specimens showed signs of mechanical failure during testing (two at 10%, six at 15%, and 23 at 20% applied strain), visible as an instant drop in the measured force response, and we excluded these data from our analyses. We provide a detailed summary relating each mechanical test (applied strain magnitude) to the patient number and OARSI grade in Table AIII.

### *Histological assessment*

We show representative images of Safranin-O stained histological slides and PicroSirius-red stained slides under polarized light in Figs. 3 and 4, respectively.

Our OARSI grading resulted in $n_{\text{OA}-1} = 19$, $n_{\text{OA}-2} = 25$, $n_{\text{OA}-3} = 14$, and $n_{\text{OA}-4} = 6$ specimens per binned group. Intra-observer agreement was $\kappa = 0.81$ for unbinned grades and $\kappa = 0.97$ for binned grades. Our PLM-CO scoring resulted in $n_5 = 5$, $n_4 = 9$, $n_3 = 15$, $n_2 = 28$, and $n_1 = 4$, with $\kappa = 0.68$ (unbinned) and $\kappa = 0.92$ (binned). For our subsequent analyses we averaged the grades/scores from both observers and assigned them to a bin (group), cf. Section Statistical analyses. Normal cartilage specimens (OA-1) had

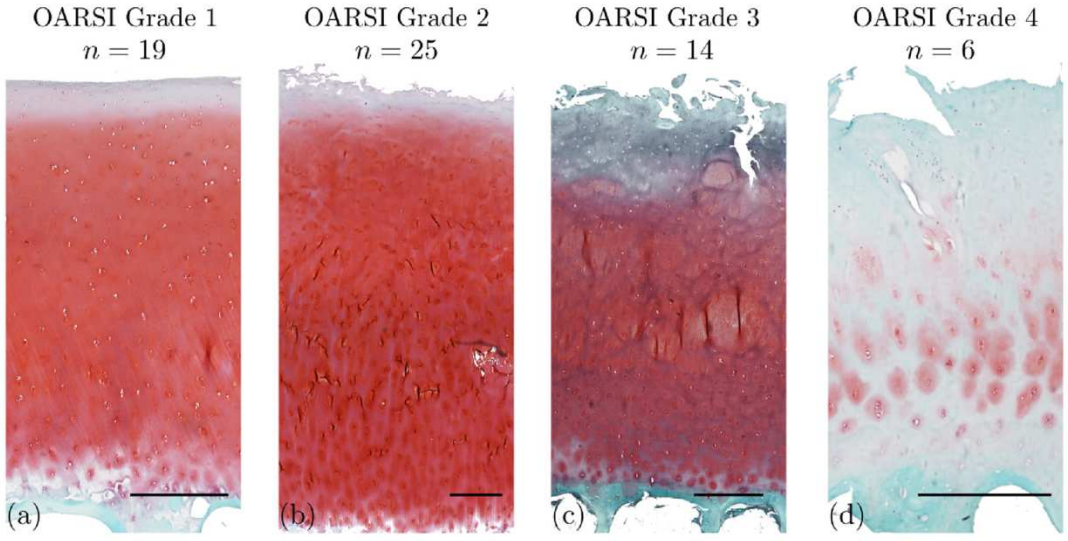


**Fig. 3.** Representative histological slides stained with Safranin-O fast green for assessing the severity of osteoarthritis using the OARSI grading method: (a) OARSI grade 1 (OA-1) – intact surface and proteoglycan (PG) content, (b) OARSI grade 2 (OA-2) – increased surface roughness and loss of PG, (c) OARSI grade 3 (OA-3) – vertical fissures and greater loss of PG, and (d) OARSI grade 4 (OA-4) – severe surface disruption and loss of PG. PG stains red. We acquired images at 35 × magnification and bars indicate 500 $\mu$m.

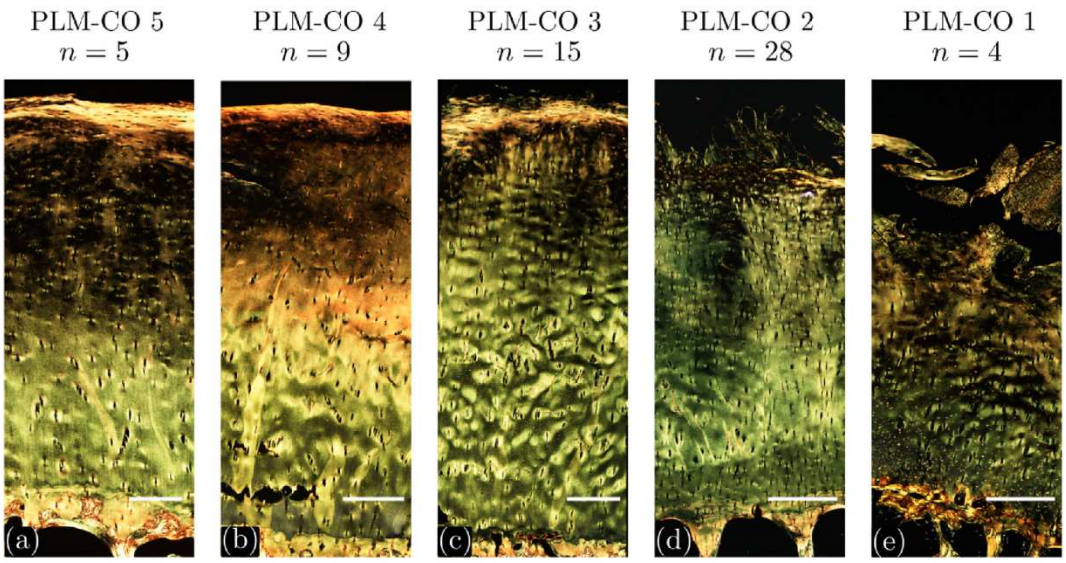


**Fig. 4.** Representative histological slides stained with PicroSirius red and visualized under polarized light for assessing the structural integrity using the PLM-CO scoring method: (a) PLM-CO score 5 – healthy zonal architecture, (b) PLM-CO score 4 – proportional but laterally heterogeneous zones, (c) PLM-CO score 3 – present but disrupted through-thickness proportions of zones, (d) PLM-CO score 2 – intact deep zone but missing other zones, and (e) PLM-CO score 1 – present but underdeveloped (˂ 50% of thickness) deep zone. Bright yellow indicates areas with fibers aligned parallel to the articular surface, black indicates randomly isotropic alignment, and bright blue-green indicates areas with fibers aligned perpendicular to the surface. We acquired images at 35 × magnification and bars indicate 500 $\mu$m.

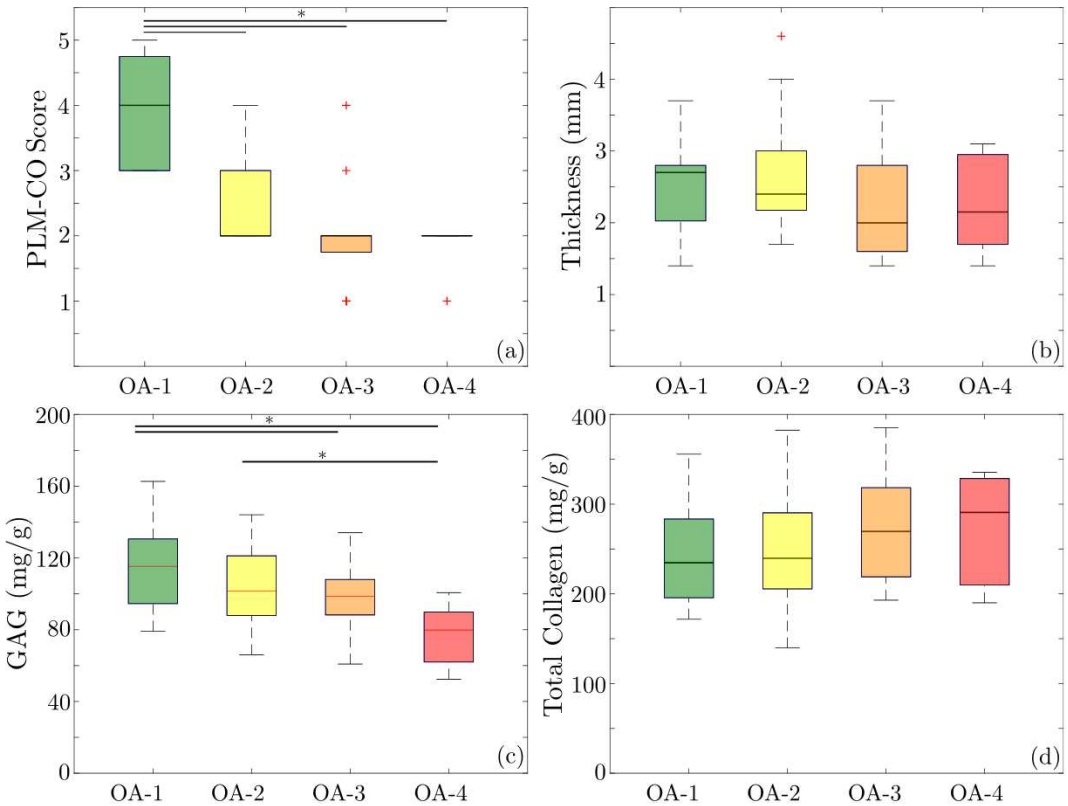


**Fig. 5.** Histological assessments and quantification of constituents in progressively osteoarthritic cartilage. (a) Boxplots of the PLM-CO scores binned by OARSI grades show higher PLM-CO scores in normal cartilage vs those with progressively advanced osteoarthritis. (b) Boxplots of cartilage thicknesses binned by OARSI grades show no significant differences between groups. (c) GAG concentration in milligram per gram wet cartilage binned by OARSI grades. (d) Collagen concentration in milligram per gram wet cartilage binned by OARSI grades. Bars labeled * indicate significant differences between groups ($P < 0.05$). Red plus signs mark outliers calculated as $Q_3 \pm 1.5(Q_3 - Q_1)$, where $Q_1$ and $Q_3$ denote the 25th and 75th percentiles of the sample data, respectively.

significantly higher PLM-CO scores vs progressively osteoarthritic specimens; see Fig. 5(a).

We found no significant differences in cartilage thicknesses binned by OARSI grades and PLM-CO scores, and compared to healthy controls (not shown); see Fig. 5(b).

*Quantification of constituents*

GAG concentration per wet weight significantly reduced with increasing OARSI grade, i.e., degeneration ($r = -0.4858$, $P < 0.0001$); see Fig. 5(c). Our pairwise comparisons showed that normal cartilage (OA-1) presents a 17% ($P = 0.0085$) and 33% ($P = 0.0007$) higher GAG concentration per wet weight than moderate (OA-3) and severely degenerated (OA-4) cartilage, respectively, and that mildly degenerated tissue (OA-2) has a 25% ($P = 0.0092$) higher concentration than severely diseased (OA-4) cartilage. Total collagen concentration by wet weight showed no significant dependence on progressing OA; see Fig. 5(d).

GAG concentration per dry weight followed qualitatively the same trends as per wet weight, i.e., a significant reduction in dry weight with increasing OARSI grade ($r = -0.4250, P = 0.0006$). Conversely, collagen concentration per dry weight with increasing OARSI grade ($r = 0.4250, P = 0.0006$).

*Mechanical anisotropy*

Data collected from specimens with a distinct SLD ($n = 52$) showed anisotropic responses in $E_{DI}$ at 5% ($P = 0.0029$), 10% ($P = 0.0425$), and 20% ($P = 0.0059$) applied strains, and $\tau_{PP}$ ($P = 0.0392$) and $G_{PE}$ ($P = 0.0044$) at 20% applied strain. If anisotropic, cartilage dissipated on average more energy and was stiffer in the SLD; see Table I. Data collected from specimens not presenting a distinct SLD ($n = 12$) did not show a dependence on direction.

In light of the mild anisotropy (if present), and to increase statistical power, we averaged the data from our two perpendicularly oriented shear tests and binned all of our data for subsequent analyses.

*Degeneration*

The Kruskal–Wallis test confirmed significant differences in mechanics among OARSI groups and vs our healthy benchmark data. We show $E_{DI}$, $\tau_{PP}$, and $G_{PE}$ summarized across all ten donors and binned by grades (including benchmarks) in Fig. 6(a–c).

**Table I**
Values of significant differences in strain-energy dissipation densities ($\Delta E_{DI}$), peak-to-peak shear stresses ($\Delta t_{PP}$), and peak effective shear modulus ($\Delta G_{PE}$) measured at shear strains $\gamma$ applied both parallel and perpendicular to the local split-line direction given as predicted median and 95% confidence interval. The percent difference is $\frac{\Delta W}{\text{median}(W_\wedge)} \times 100$, where median($W_\wedge$) is the median value from data in the perpendicular direction

| $\gamma$ (%) | 5 | 10 | 20 |
|---|---|---|---|
| % | 15.57 | 10.20 | 10.80 |
| $\Delta E_{DI}$ (mJ/mm$^3$) | 0.1099 | 0.2791 | 1.056 |
| CI | (0.0422,0.1763) | (0.02051,0.5377) | (0.02124,2.091) |
| $P$ | 0.0019 | 0.035 | 0.0327 |
| % | | | 14.74 |
| $\Delta t_{PP}$ (kPa) | | | 34.94 |
| CI | – | – | (3.556,66.33) |
| $P$ | | | 0.0308 |
| % | | | 23.95 |
| $\Delta G_{PE}$(kPa) | | | 253.9 |
| CI | – | – | (88.13,419.7) |
| $P$ | | | 0.0045 |

Within the OA groups we found that severely degenerated cartilage (OA-4) dissipated less strain energy and showed reduced peak-to-peak stresses and reduced peak-effective shear moduli vs normal OA tissue (OA-1). Healthy (control) load-bearing cartilage ($HL_0$) dissipated significantly more strain energy vs any cartilage originating from a diseased knee (OA-1 to -4). Non-load-bearing cartilage (HN) dissipated more energy than mildly to severely degenerated cartilage (OA-2 and -4) at some applied strain levels. Peak-to-peak shear stresses $\tau_{PP}$ from healthy load-bearing cartilage ($HL_0$) were significantly higher vs those from mildly to severely degenerated cartilage (OA-2 and -4). Peak-to-peak shear stresses were not significantly different between healthy non-load-bearing cartilage (HN) and degenerated cartilage (any). Healthy load-bearing cartilage was only significantly stiffer ($G_{PE}$) than severely degenerated cartilage at larger applied strains (15–20%). Normal cartilage from an OA joint (OA-1) had a significantly stiffer response than severely degenerated cartilage at 5, 15, and 20% applied strain and was only stiffer than cartilage with mild (OA-2) and advanced degeneration at 5% and 15%, respectively.

In Appendix (A), we report all the quantitative data for Fig. 6(a–c) in Table AIV, and percent and absolute differences of shear strain-energy dissipations $E_{DI}$, peak-to-peak shear stresses $\tau_{PP}$, and peak effective shear moduli $G_{PE}$ in Tables AV to AVII.

*Structural integrity*

The Kruskal–Wallis test confirmed significant differences in mechanics among groups binned by PLM-CO score. We show $E_{DI}$, $\tau_{PP}$, and $G_{PE}$ summarized across all ten donors and binned by PLM-CO scores in Fig. 6(d–f). All mechanical measures ($E_{DI}$, $\tau_{PP}$, and $G_{PE}$) were 30–40% higher with the presence of zonal structure, indicated by a higher PLM-CO score, consistent over all applied strain magnitudes.

In Appendix (A), we report all the quantitative data for Fig. 6(d–f) in Table AIV.

*Collagen and proteoglycan content, thickness, and age*

Total collagen content by wet weight, specimen thickness, and patient age (as independent factors) did not correlate with any mechanical measures ($E_{DI}$, $\tau_{PP}$, $G_{PE}$). All mechanical measures, except $E_{DI}$ at 5% and 10% applied shear strain, showed a weak to moderate correlation with GAG content; see Table II. GAG concentration by dry weight shows qualitatively the same correlations with the respective mechanical measures as GAG by wet weight. While all mechanical measures increase with increasing GAG concentration, they similarly reduce with increasing collagen content.

Thickness decreased significantly with age ($r = -0.7041$, $P < 0.0001$).

## Discussion

This study is the first to quantify the mechanical properties of progressively osteoarthritic human articular cartilage undergoing large shear strains (up to 20%). Cartilage shows a nonlinear stress–strain relationship with a distinct hysteresis for all magnitudes of applied strain (cf. Fig. 2), where shear strain-energy dissipation, peak-to-peak shear stress, and peak effective shear modulus progressively reduce with advancing OA.

*Histological assessment*

We found good inter-observer agreement for OARSI grades and PLM-CO scores and had excellent agreement when comparing the

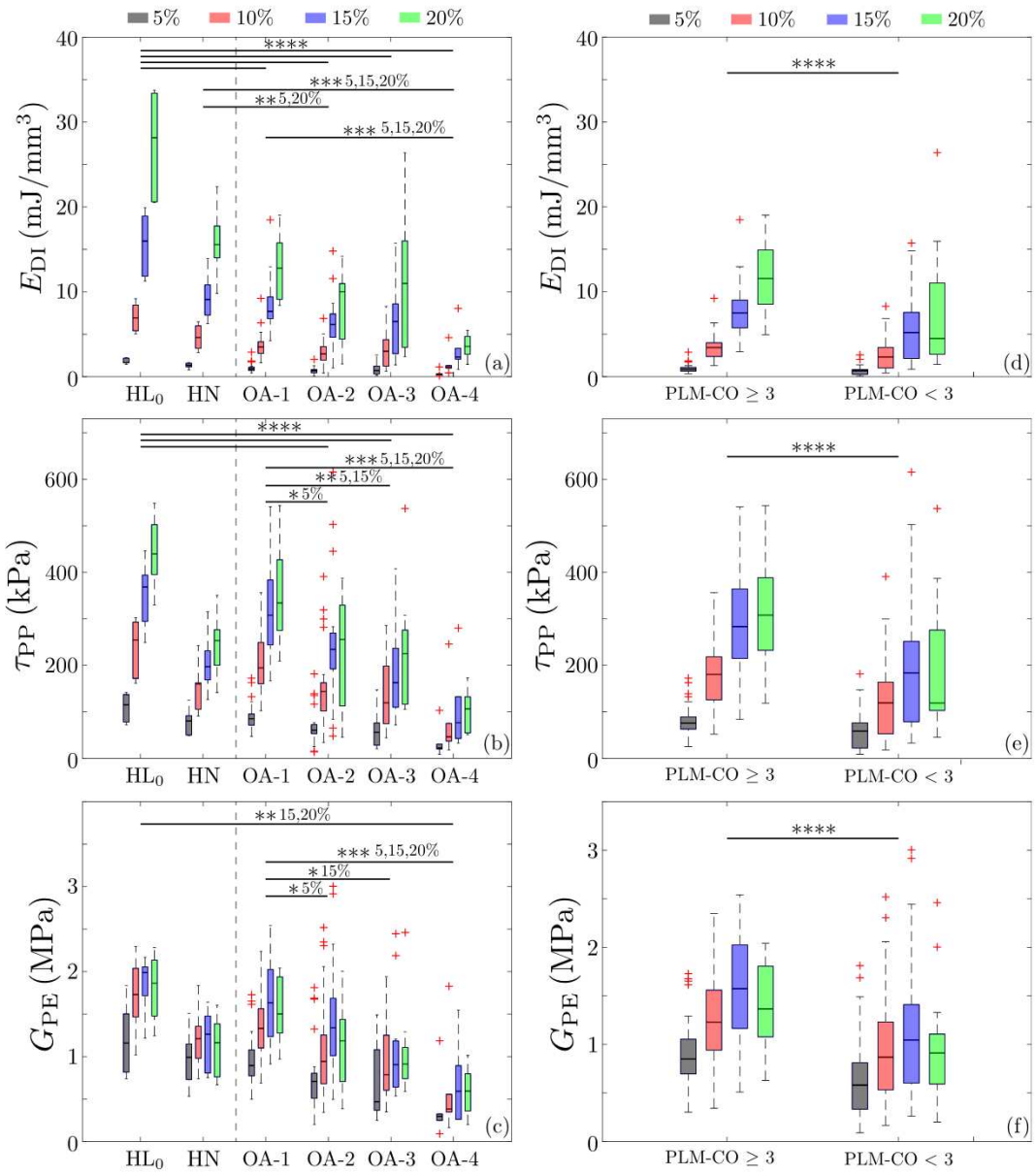


**Fig. 6.** Box plots of the (a), (d) strain-energy dissipation densities ($E_{DI}$), (b), (e) peak-to-peak shear stresses ($\tau_{PP}$), and (c), (f) peak effective shear moduli ($G_{PE}$) at all magnitudes of applied strain across all donors and binned by OARSI grades (OA-1 to -4) in (a–c) and binned by PLM-CO scores ($\geq 3$ or $<3$) in (d–f). As a benchmark, we include data from load-bearing (HL$_0$) and non-load-bearing (HN) locations within healthy young joints[21]. Bars labeled * indicate significant differences between groups ($P < 0.05$). The number of * indicates significance at that number of strain magnitudes, and we indicate the significant strain magnitudes, cf. Appendix (A). Red plus signs mark outliers calculated as $Q_3 \pm 1.5(Q_3 - Q_1)$, where $Q_1$ and $Q_3$ denotes the 25th and 75th percentiles of the sample data, respectively.

**Table II**
Pearson's correlation coefficient $r$ and $P$-values for significant correlations between our mechanical measures ($E_{DI}$, $\tau_{PP}$, $G_{PE}$) and GAG concentration

| $\gamma$ (%) | | 5 | 10 | 15 | 20 |
|---|---|---|---|---|---|
| $E_{DI}$ | $r$ | – | – | 0.4342 | 0.4593 |
| | $P$ | | | 0.0016 | 0.0107 |
| $\tau_{PP}$ | $r$ | 0.4038 | 0.4541 | 0.4914 | 0.5973 |
| | $P$ | 0.0011 | 0.0003 | 0.0003 | 0.0005 |
| $G_{PE}$ | $r$ | 0.3717 | 0.3975 | 0.4034 | 0.5424 |
| | $P$ | 0.0029 | 0.0020 | 0.0037 | 0.0020 |

binned groups (Section Statistical analyses). In light of the heterogeneous intra-joint progression of OA, we used OARSI grade as a local measure of cartilage degeneration, vs the OARSI score, which also includes a joint-scale measure of OA. Utilizing the OARSI grading method also allowed us to resolve early stages of OA[15]. Different quantification methods do show strong correlations, e.g., OARSI vs Mankin[28], Mankin vs ICRS[13], but they differ in terminology and definitions of early-stage OA. For the subsequent comparisons, we interpret published results in the context of the OARSI grade.

We determined the PLM-CO scores based on digital images, and if not clearly distinguishable, we directly observed slides under the microscope, better allowing us to rotate them. We oriented the slides shown in Fig. 4 to emphasize the main features for PLM-CO scoring. We did not post-process (i.e., enhance contrast or manipulate color) these PLM images, cf. Changoor *et al.*[25]. Binning our PLM-CO scores by presence/absence of zonal structure, resulted in two groups of equal size ($\geq 3$ or $<3$), improving statistical power and allowing us to investigate the general influence of collagen architecture. Our approach does not allow us to distinguish between different stages of structural degeneration.

*Quantification of constituents*

Both the GAG and total collagen content per wet weight we report are within ranges reported previously[10,29,1], as is the progression of these with OA, i.e., a progressive reduction in GAG concentration and no significant change in collagen concentration[30]. The combined weight of GAGs and collagen accounts for the strong majority of the total dry weight of cartilage[31,32]. Thus, statistics based on the constituents per dry weight does not allow independent observations on the effects of GAG and collagen concentrations, i.e., if GAG concentration reduces with degeneration, collagen concentration must increase. The concentration of water changes in cartilage as a function of OA[1], thus concentrations of the constituents calculated by wet weight carry essential information regarding the integrity of cartilage. Fixation procedures likely cause collagen cross-linking and may compromise the capability of cartilage to rehydrate[33–35]. None-the-less all of our samples underwent the same treatment, i.e., fixation, decalcification, embedding, and storage; thus our results are self consistent.

*Mechanical anisotropy*

Shear strain energy dissipation correlated significantly with the SLD at all magnitudes of applied shear strain (except at 15%), indicating that dissipated energy is linked to organization of the collagen network. The mechanical measures $\tau_{PP}$ and $G_{PE}$ also correlated significantly with the SLD at larger strains (20%), similar to healthy control tissue[21]. Quantifying mechanical anisotropy by OARSI grade (results not shown) did not reveal consistent trends. Anisotropy is more pronounced at the articular surface of healthy cartilage[36] due to the pronounced fiber alignment in the SZ. Using cartilage specimens tested in unconfined compression Robinson *et al.*[12] reported a significant reduction in anisotropy near the articular surface with increasing degeneration. Our shear test may not reveal this change since we restrict the SZ in our experiment. Of the 12 specimens without a clear local SLD, five presented OARSI grade 2, five OARSI grade 4, and two OARSI grade 3, thus all showed signs of degeneration. However, this is not necessarily a sign of degeneration as even within healthy joints regions may show an isotropic fiber distribution, i.e., no apparent SLD[37].

*Degeneration*

Differences in the shapes of pieces of condyles obtained from TKA may introduce uncertainty in determining load-bearing regions within the lateral condyles. Thus, we chose to provide context for our mechanical results with upper and lower bounds determined in our previous study using healthy cartilage[21].

Energy dissipation in cartilage stems from interactions of the fluid and solid phase, and from GAG-GAG and GAG-collagen interactions[20]. The quasi-static design of our experiment excludes fluid–solid interactions; thus our reported energy dissipation originates from solid–solid interactions only. We found a reduction in $E_{DI}$ up to 80% (cf. Table A5) in severely degenerated (OA-4) vs normal (OA-1) cartilage, consistent with Abdel-Sayed *et al.*[38]. Using enzymatic digestion as a model for OA, other researchers found similar reductions in viscous effects: e.g., in coefficients of restitution[39], phase-shift angles[20], stress-relaxation times[40], and storage and loss moduli[41]. In contrast, Griffin *et al.*[42] reported an increase in energy dissipation with PG depletion. This contradiction might be explained by differences in the test and enzymatic treatment protocols. Importantly, we found that even cartilage with a normal appearance in structure and composition (OA-1) dissipated ~50% less energy than healthy (control) load-bearing cartilage ($HL_0$). In comparison to healthy non-load-bearing cartilage (HN), mildly (OA-2) and severely (OA-4) degenerated cartilage showed a strain-dependent reduction in dissipated energy of ~50% and 70% respectively. Furthermore, energy dissipation may play an important role in maintaining an optimum temperature for chondrocytes and chondrogenic expression[43]. Thus a strong reduction in the ability of cartilage to dissipate energy in early-stage OA may initiate and/or accelerate a cascade of degeneration.

Stress- and stiffness-based measures allowed us to differentiate degenerated cartilage (OA-2 to -4) as significantly softer than healthy load-bearing ($HL_0$) and normal (OA-1) cartilage. Our results are consistent with the cartilage mechanics literature investigating stress and stiffness and the general finding that those metrics are not sufficient to detect the early onset of OA or to distinguish consistently among different levels of degeneration, e.g.,[13,44,39,14]. Differences in the mean ages of our diseased specimens and our healthy controls might contribute to the observed behaviors; however, two subsequent studies, one on the effects of age[45] and one on disease[30], suggest that the latter accounts for approximately 80% of the observed mechanical softening.

*Structural integrity*

All of our reported mechanical measures decrease 30–40% when the zonal architecture of cartilage becomes compromised. However, all specimens obtained from TKAs (OA-1 to -4) showed signs of remodeling in the SZ, i.e., a PLM score $<5$[46]. showed that energy dissipation is highest near the transition from SZ to MZ. Thus, the ~50% decrease in energy dissipation that we report between healthy load-bearing ($HL_0$) and normal (OA-1) cartilage from TKAs may originate from minute changes in the zonal architecture near the articular surface.

Desrochers *et al.*[47] found, using atomic force microscopy, that the time-dependent mechanics of cartilage under cyclic compression are sensitive to changes associated with early-stage OA, and they concluded that changes within the collagen network have a greater effect than changes in the composition. We showed the same effects by macro-scale measurements, thus highlighting the potential for clinical application. Current instruments for arthroscopic indentation lack sensitivity to detect early-stage OA[48,49]. If such instruments could be adapted to measure both the loading and unloading response, a measure of energy dissipation may realize this goal.

*Collagen and proteoglycan content, thickness, and age*

We found a weak to moderate correlation of all our mechanical measures, except $E_{DI}$ at strain levels 5% and 10%, with GAG content. The strong negative fixed charge of GAG molecules attracts fluid to increase the osmotic pressure within the tissue and pre-tension the collagen network. Thus both the network of collagen and the corresponding bulk tissue response appears stiffer[50]. We did not find correlations between any of our mechanical measures and total

collagen content, and collagen content did not significantly change with progressing degeneration. This result emphasizes that collagen structure and the zonal architecture play greater roles in cartilage mechanics than does collagen content[47].

We found no correlations between any of our mechanical measures, nor the OARSI grades, and the thicknesses of our specimens. This result confirms that specimen thickness is a poor predictor for cartilage health, cf. Guermazi *et al.*[51]. N.B. specimen thickness can still be used to observe the progression of OA in longitudinal studies if a healthy baseline is established[52]. We did find that the reduction in specimen thickness correlated with age.

We did not find correlations between any of our mechanical measures and age. Thus, OA-associated degeneration has a greater effect than age on the mechanical behavior of cartilage, cf. Temple *et al.*[45].

### *Limitations and outlook*

We included only tissue from lateral femoral condyles although degeneration generally presents first in the medial femoral condyle[53]. However, the mechanical properties of cartilage from the medial and lateral condyles are not significantly different[54,27], thus our findings should apply to both lateral and medial femoral condyles.

Our mechanical results do not represent *in vivo* loading rates, where healthy cartilage can generate substantial hydrostatic interstitial fluid pressure. However, our results allow us to decouple the mechanical responses (solid vs fluid) and to investigate changes in the bulk properties of the solid constituents, thus identifying changes in the solid matrix that may be masked by alterations of the permeability[39]. Cartilage stiffness, in both tension and compression, is rate dependent but reaches a plateau if the rate of applied deformation is sufficiently slow[55,56]. We found that rate to be 75 $\mu$m/min for healthy control cartilage under simple shear, Maier et al.[21].

Our testing device did not allow us to identify the origins of mechanical failures (we excluded these data from our analyses). Inspections of the specimens confirmed that failures always occurred near the articular surface, but we could not distinguish between failure of the very soft cartilage near the surface and the gluing interface itself.

We found that the progression of OA significantly changes the mechanical responses of articular cartilage undergoing large-strain shear deformations. Our results suggest that a reduction in energy dissipation can be detected by bulk-tissue testing, and that this reduction precedes visible signs of degeneration. This significant reduction is associated with remodeling of the collagen network and with alterations in the zonal architecture, rather than with changes in cartilage composition. Our results highlight the potential of energy dissipation, as opposed to stress- or stiffness-based measures, as a marker to diagnose early-stage OA.

## Author contributions

FM contributed to conception and design; prepared specimens and conducted the experiments; analyzed and interpreted data; participated in drafting the article and revising it critically; and gave final approval of the version submitted. CGL contributed tissues; revised the article critically; and gave final approval of the version submitted. DMP oversaw the project; contributed to conception and design; analyzed and interpreted data; participated in drafting the article and revising it critically; and gave final approval of the version submitted.

## Conflicts of interest

We have no conflicts of interest to report.

## Role of the funding source

We gratefully acknowledge funding from the National Science Foundation (NSF) 1662429. The NSF had no involvement in the study design; in collection, analysis and interpretation of data; in the writing of the manuscript; and in the decision to submit the manuscript for publication.

## Acknowledgments

We thank many orthopedic surgeons from Hartford Healthcare for collecting cartilage from TKAs. We also thank Lauren Marshall (LM) and Victoria Blair for assisting with PLM-CO scoring, and GAG and collagen assays respectively. We thank the Statistical Consulting Services (SCS) at the University of Connecticut for assistance with our statistical analyses.

## Appendix A

We provide a detailed summary relating each mechanical test (applied strain magnitude) to the patient number and OARSI grade used for statistical analyses in Table AIII.

**Table AIII**
Detailed summary relating each mechanical test (applied strain magnitude) to the patient number and OARSI grade used for statistical analyses. A decreasing number of tests across one row indicates that specimen(s) failed mechanically. The total number of tests shown at the bottom is the number of data available for statistical analyses at each strain magnitude

| Patient | OARSI Grade | Specimens at applied strain $\gamma$ (%) | | | |
|---|---|---|---|---|---|
| | | 5 | 10 | 15 | 20 |
| 1 | 1 | 1 | 1 | 1 | 1 |
| | 2 | 2 | 2 | 1 | 1 |
| | 3 | 2 | 2 | 2 | 2 |
| | 4 | 1 | 1 | 1 | 1 |
| 2 | 1 | 3 | 3 | 2 | 1 |
| | 2 | 2 | 2 | 2 | 1 |
| | 4 | 2 | 2 | 2 | 2 |
| 3 | 1 | 2 | 2 | 1 | 0 |
| | 2 | 2 | 2 | 1 | 0 |
| | 3 | 4 | 3 | 3 | 2 |
| 4 | 1 | 2 | 2 | 2 | 2 |
| | 2 | 2 | 2 | 2 | 2 |
| 5 | 1 | 1 | 1 | 1 | 0 |
| | 2 | 5 | 4 | 4 | 2 |
| | 3 | 1 | 1 | 0 | 0 |
| | 4 | 1 | 1 | 1 | 0 |
| 6 | 1 | 1 | 1 | 1 | 0 |
| | 2 | 2 | 2 | 2 | 1 |
| | 3 | 2 | 2 | 2 | 2 |
| 7 | 1 | 2 | 2 | 2 | 1 |
| | 2 | 3 | 3 | 3 | 0 |
| | 3 | 1 | 1 | 1 | 0 |
| | 4 | 2 | 2 | 2 | 2 |
| 8 | 1 | 4 | 4 | 4 | 3 |
| | 2 | 2 | 2 | 2 | 2 |
| | 3 | 1 | 1 | 1 | 0 |
| 9 | 2 | 4 | 4 | 3 | 0 |
| | 3 | 3 | 3 | 3 | 3 |
| 10 | 1 | 3 | 3 | 3 | 2 |
| | 2 | 1 | 1 | 1 | 0 |
| Total Number $n$ | | 64 | 62 | 56 | 33 |

We report the quantitative data for shear strain-energy dissipation $E_{DI}$, peak-to-peak shear stresses $\tau_{PP}$, and peak effective shear modulus $G_{PE}$ in Table AIV, and percent and absolute differences of these in Tables AV to AVII.

**Table AIV**
Shear strain-energy dissipation densities ($E_{DI}$), peak-to-peak shear stresses ($\tau_{PP}$), and peak effective shear moduli ($G_{PE}$) given as median and interquartile range [$Q_1$,$Q_3$] at all magnitudes of applied strain across all donors and binned by OARSI grades (OA-1 to −4) and PLM-CO scores ($\geq 3$ or $<3$)

| $\gamma$ (%) | | OARSI Grade | | | | PLM-CO Score | |
|---|---|---|---|---|---|---|---|
| | | 1 | 2 | 3 | 4 | $\geq 3$ | $<3$ |
| 5 | $E_{DI}$ | 0.9143 | 0.7188 | 0.7274 | 0.2990 | 0.8568 | 0.6986 |
| | (mJ/mm$^3$) | [0.7216,1.105] | [0.4743,0.8524] | [0.3220,1.254] | [0.2645,0.3392] | [0.6641,1.085] | [0.2875,0.8481] |
| | $\tau_{PP}$ | 85.24 | 60.45 | 56.08 | 22.48 | 76.09 | 58.60 |
| | (kPa) | [71.65,95.53] | [53.42,72.58] | [28.37,76.05] | [20.39,30.54] | [63.09,89.38] | [22.48,76.47] |
| | $G_{PE}$ | 894.0 | 707.0 | 468.0 | 297.0 | 848.3 | 580.8 |
| | (kPa) | [773.0,1079] | [509.2,802.9] | [366.6,1081] | [247.0,323.7] | [696.4,1052] | [332.8,810.1] |
| 10 | $E_{DI}$ | 3.516 | 2.680 | 2.990 | 1.098 | 3.433 | 2.326 |
| | (mJ/mm$^3$) | [2.760,4.111] | [1.938,3.548] | [1.256,4.370] | [1.018,1.305] | [2.383,3.988] | [1.024,3.444] |
| | $\tau_{PP}$ | 194.7 | 143.8 | 119.7 | 46.46 | 180.5 | 119.5 |
| | (kPa) | [160.6,249.0] | [102.0,162.6] | [74.55,198.5] | [37.32,75.29] | [126.0,218.5] | [53.14,163.8] |
| | $G_{PE}$ | 1331 | 942.3 | 786.7 | 381.1 | 1230 | 868.3 |
| | (kPa) | [1101,1563] | [680.7,1253] | [602.9,1251] | [346.7,555.1] | [939.9,1559] | [532.5,1230] |
| 15 | $E_{DI}$ | 7.699 | 6.147 | 6.509 | 2.326 | 7.515 | 5.201 |
| | (mJ/mm$^3$) | [6.828,9.404] | [4.633,7.397] | [2.715,8.573] | [ 2.076,3.341] | [5.764,9.005] | [2.151,7.573] |
| | $\tau_{PP}$ | 307.7 | 234.6 | 162.7 | 76.63 | 283.6 | 183.8 |
| | (kPa) | [244.3,383.5] | [192.4,269.7] | [110.1,236.9] | [42.64, 132.5] | [214.9,364.5] | [79.00,251.9] |
| | $G_{PE}$ | 1634 | 1338 | 904.8 | 589.7 | 1574 | 1045 |
| | (kPa) | [1235,2025] | [1011,1685] | [640.1,1183] | [260.8,891.7] | [1165,2025] | [600.8,1410] |
| 20 | $E_{DI}$) | 12.79 | 10.03 | 10.99 | 3.559 | 11.55 | 4.508 |
| | (mJ/mm$^3$) | [9.111,15.76] | [4.429,10.97] | [3.473,16.00] | [2.662,4.746] | [8.522,14.94] | [2.652,11.04] |
| | $\tau_{PP}$ | 334.1 | 255.4 | 225.5 | 106.4 | 308.0 | 118.8 |
| | (kPa) | [275.2,427.1] | [113.1,329.1] | [116.7,275.9] | [55.00,132.1] | [232.43,388.35] | [103.1,275.9] |
| | $G_{PE}$ | 1502 | 1185 | 910.1 | 592.9 | 1366 | 910.1 |
| | (kPa) | [1277,1938] | [705.2,1437] | [740.5,1106] | [360.2,795.7] | [1078,1804] | [591.6,1106] |

**Table AV**
Relative and absolute differences in shear strain-energy dissipation density ($E_{DI}$) of normal cartilage from TKAs and healthy controls (rows) versus cartilage with progressing OA (columns). OA-1 to −4 denotes the corresponding OARSI grade, $HL_0$ and HN denote healthy controls from load-bearing (under 0° knee flexion) and non-load-bearing regions, respectively. The percent difference is calculated as $\frac{\Delta E_{DI}}{\text{median}(E_{DI,ref})} \times 100$. CI denotes the 95% confidence interval

| $\Delta E_{DI}$ | | | Compared to OARSI grade | | | |
|---|---|---|---|---|---|---|
| $\gamma$ (%) | Reference | | OA-1 | OA-2 | OA-3 | OA-4 |
| 5 | OA-1 | % | | | | 66.04 |
| | | (mJ/mm$^3$) | – | – | – | 0.6038 |
| | | CI | | | | (0.3565,0.8510) |
| | | $P$ | | | | 0.0083 |
| | $HL_0$ | % | 51.70 | 63.83 | 58.85 | 89.93 |
| | | (mJ/mm$^3$) | 0.8595 | 1.061 | 0.9783 | 1.495 |
| | | CI | (0.5170,1.202) | (0.6895,1.433) | (0.3744,1.582) | (1.035,1.955) |
| | | $P$ | 0.0068 | $<0.0001$ | 0.0032 | 0.0051 |
| | HN | % | | 42.50 | | 66.67 |
| | | (mJ/mm$^3$) | – | 0.5770 | – | 0.9051 |
| | | CI | | (0.2060,0.9480) | | (0.4400,1.370) |
| | | $P$ | | 0.0035 | | 0.0082 |
| 10 | $HL_0$ | % | 48.01 | 60.69 | 56.47 | 84.71 |
| | | (mJ/mm$^3$) | 3.327 | 4.206 | 3.913 | 5.871 |
| | | CI | (1.662,4.992) | (2.828,5.583) | (1.836,5.990) | (3.765,7.977) |
| | | $P$ | 0.0030 | $<0.0001$ | 0.0010 | 0.0051 |
| | HN | % | | 40.31 | | |
| | | (mJ/mm$^3$) | – | 1.866 | – | – |
| | | CI | | (0.5195,3.212) | | |
| | | $P$ | | 0.0084 | | |
| 15 | OA-1 | % | | | | 65.049 |
| | | (mJ/mm$^3$) | – | – | – | 5.008 |
| | | CI | | | | (2.749,7.268) |
| | | $P$ | | | | 0.0045 |
| | $HL_0$ | % | 46.59 | 58.48 | 58.19 | 78.11 |
| | | (mJ/mm$^3$) | 7.442 | 9.340 | 9.294 | 12.48 |
| | | CI | (3.586,11.30) | (6.191,12.49) | (4.933,13.66) | (8.518,16.44) |
| | | $P$ | | $<0.0001$ | 0.0004 | $<0.0001$ |
| | HN | % | | | | 68.63 |
| | | (mJ/mm$^3$) | – | – | – | 6.247 |
| | | CI | | | | (2.864,9.631) |

(*continued on next page*)

**Table AV** (*continued*)

| $\Delta E_{DI}$ | | | Compared to OARSI grade | | | |
|---|---|---|---|---|---|---|
| $\gamma$ (%) | Reference | | OA-1 | OA-2 | OA-3 | OA-4 |
| | | *P* | | | | 0.0021 |
| 20 | OA-1 | % | | | | 72.19 |
| | | (mJ/mm$^3$) | – | – | – | 9.236 |
| | | CI | | | | (5.210,13.26) |
| | | *P* | | | | 0.0004 |
| | $HL_0$ | % | 51.80 | 68.21 | 59.07 | 84.60 |
| | | (mJ/mm$^3$) | 14.59 | 19.21 | 16.63 | 23.82 |
| | | CI | (8.945,20.23) | (13.55,24.86) | (8.272,24.99) | (17.68,29.96) |
| | | *P* | 0.0001 | $<0.0001$ | 0.0009 | $<0.0001$ |
| | HN | % | | 48.98 | | 78.66 |
| | | (mJ/mm$^3$) | – | 7.620 | – | 12.24 |
| | | CI | | (2.778,12.46) | | (7.770,16.70) |
| | | *P* | | 0.0047 | | 0.0002 |

**Table AVI**
Relative and absolute differences in peak-to-peak shear stresses $\tau_{PP}$ of normal cartilage from TKAs and healthy controls (rows) versus cartilage with progressing OA (columns). OA-1 to −4 denotes the corresponding OARSI grade, $HL_0$ and HN denote healthy controls from load-bearing (under 0° knee flexion) and non-load-bearing regions, respectively. The percent difference is calculated as $\frac{\Delta\tau_{PP}}{\text{median}(\tau_{PP,ref})} \times 100$. CI denotes the 95% confidence interval

| $\Delta\tau_{PP}$ | | | Compared to OARSI grade | | |
|---|---|---|---|---|---|
| $\gamma$ (%) | Reference | | OA-2 | OA-3 | OA-4 |
| 5 | OA-1 | % | | 37.84 | 62.29 |
| | | (kPa) | – | 32.26 | 53.09 |
| | | CI | | (9.190,55.32) | (29.43,76.76) |
| | | *P* | | 0.0083 | 0.0083 |
| | $HL_0$ | % | 38.41 | 43.81 | 67.08 |
| | | (kPa) | 44.15 | 50.36 | 77.11 |
| | | CI | (11.27,77.04) | (13.28,87.44) | (34.22,120.0) |
| | | *P* | 0.0064 | 0.0106 | 0.0202 |
| 10 | OA-1 | % | | | 63.67 |
| | | (kPa) | – | – | 124.0 |
| | | CI | | | (59.34,188.6) |
| | | *P* | | | 0.0069 |
| | $HL_0$ | % | 35.29 | 42.25 | 63.38 |
| | | (kPa) | 89.86 | 107.6 | 161.4 |
| | | CI | (14.73,165.0) | (32.92,182.3) | (10.79,101.9) |
| | | *P* | 0.0166 | 0.0074 | 0.0202 |
| 15 | OA-1 | % | | 40.78 | 66.75 |
| | | (kPa) | – | 125.5 | 205.4 |
| | | CI | | (39.86,211.2) | (104.4,306.4) |
| | | *P* | | 0.0058 | 0.0004 |
| | $HL_0$ | % | 29.87 | 45.22 | 66.91 |
| | | (kPa) | 110.1 | 166.6 | 246.5 |
| | | CI | (14.51,205.6) | (60.39,272.8) | (141.1,351.8) |
| | | *P* | 0.0239 | 0.0044 | 0.0004 |
| 20 | OA-1 | % | | | 75.47 |
| | | (kPa) | – | – | 252.1 |
| | | CI | | | (137.7,366.4) |
| | | *P* | | | 0.0005 |
| | $HL_0$ | % | 48.42 | 49.16 | 77.66 |
| | | (kPa) | 212.9 | 216.1 | 341.4 |
| | | CI | (92.42,333.4) | (81.40,350.9) | (250.3,432.5) |
| | | *P* | 0.0021 | 0.0042 | $P<0.0001$ |

**Table AVII**
Relative and absolute differences in peak-effective shear moduli $G_{PE}$ of normal cartilage from TKAs and healthy controls (rows) versus cartilage with progressing OA (columns). OA-1 to −4 denotes the corresponding OARSI grade, $HL_0$ and HN denote healthy controls from load-bearing (under 0° knee flexion) and non-load-bearing regions, respectively. The percent difference is calculated as $\frac{\Delta G_{PE}}{\text{median}(G_{PE,ref})} \times 100$. CI denotes the 95% confidence interval

| $\Delta G_{PE}$ | | | Compared to OARSI grade | | |
|---|---|---|---|---|---|
| $\gamma$ (%) | Reference | | OA-2 | OA-3 | OA-4 |
| 5 | OA-1 | % | 26.98 | | 67.15 |
| | | (kPA) | 241.2 | – | 600.3 |
| | | CI | (61.93,420.6) | | (387.2,813.5) |
| | | *P* | 0.0080 | | 0.0083 |
| 15 | OA-1 | % | | 36.21 | 57.40 |
| | | (kPA) | – | 591.5 | 937.9 |
| | | CI | | (129.0,1054) | (427.5,1448) |
| | | *P* | | 0.0096 | 0.0010 |
| | $HL_0$ | % | | | 58.63 |
| | | (kPA) | – | – | 1165 |
| | | CI | | | (624.2,1706) |
| | | *P* | | | 0.0007 |
| 20 | OA-1 | % | | | 64.39 |
| | | (kPA) | – | – | 967.0 |
| | | CI | | | (510.7,1423) |
| | | *P* | | | 0.0007 |
| | $HL_0$ | % | | | 65.61 |
| | | (kPA) | – | – | 1223 |
| | | CI | | | (723.8,1721) |
| | | *P* | | | 0.0004 |

## References


1. Buckwalter JA, Mankin HJ, Grodzinsky AJ. Articular cartilage and osteoarthritis. Instr Course Lect 2005;54:465–80.
2. Adams ME, Brandt KD. Hypertrophic repair of canine articular cartilage in osteoarthritis after anterior cruciate ligament transection. J Rheumatol 1991;18:428–35.
3. Goldring MB. The role of the chondrocyte in osteoarthritis. Arthritis Rheum 2000;43:1916–26.
4. Roach HI, Yamada N, Cheung KSC, Tilley S, Clarke NMP, Oreffo ROC, *et al.* Association between the abnormal expression of matrix-degrading enzymes by human osteoarthritic chondrocytes and demethylation of specific CpG sites in the promoter regions. Arthritis Rheum 2005;52:3110–24.
5. Setton LA, Mow VC, Howell DS. Mechanical behavior of articular cartilage in shear is altered by transection of the anterior cruciate ligament. J Orthop Res 1995;13:473–82.
6. Hwang J, Bae WC, Shieu W, Lewis CW, Bugbee WD, Sah RL. Increased hydraulic conductance of human articular cartilage and subchondral bone plate with progression of osteoarthritis. Arthritis Rheum 2008;58:3831–42.
7. Changoor A, Tran-Khanh N, Methot S, Garon M, Hurtig MB, Shive MS, *et al.* A polarized light microscopy method for accurate and reliable grading of collagen organization in cartilage repair. Osteoarthritis Cartilage 2011;19:126–35.
8. Moger CJ, Barrett R, Bleuet P, Bradley DA, Ellis RE, Green EM, *et al.* Regional variations of collagen orientation in normal and diseased articular cartilage and subchondral bone determined using small angle X-ray scattering (SAXS). Osteoarthritis Cartilage 2007;15:682–7.
9. Goldring MB, Goldring SR. Articular cartilage and subchondral bone in the pathogenesis of osteoarthritis. Ann N Y Acad Sci 2010;1192:230–7.
10. Franz T, Hasler EM, Hagg R, Weiler C, Jakob RP, Mainil-Varlet P. In situ compressive stiffness, biochemical composition, and structural integrity of articular cartilage of the human knee joint. Osteoarthritis Cartilage 2001;9:582–92.
11. Garcia-Seco E, Wilson DA, Cook JL, Kuroki K, Kreeger JM, Keegan KG. Measurement of articular cartilage stiffness of the femoropatellar, tarsocrural, and metatarsophalangeal joints in horses and comparison with biochemical data. Vet Surg 2005;34:571–8.
12. Robinson DL, Kersh ME, Walsh NC, Ackland DC, de Steiger RN, Pandy MG. Mechanical properties of normal and osteoarthritic human articular cartilage. J Mech Behav Biomed Mater 2016;61:96–109.
13. Kleemann RU, Krocker D, Cedraro A, Tuischer J, Duda GN. Altered cartilage mechanics and histology in knee osteoarthritis: relation to clinical assessment (ICRS Grade). Osteoarthritis Cartilage 2005;13:958–63.
14. Kumar R, Pierce DM, Isaksen V, de Lange Davies C, Drogset JO, Lilledahl MB. Comparison of compressive stress-relaxation behavior in osteoarthritic (ICRS graded) human articular cartilage. Int J Mol Sci 2018;19:E413.
15. Pritzker KPH, Gay S, Jimenez SA, Ostergaard K, Pelletier JP, Revell PA, *et al.* Osteoarthritis cartilage histopathology: grading and staging. Osteoarthritis Cartilage 2006;14:13–29.
16. Chan DD, Cai L, Butz KD, Trippel SB, Nauman EA, Neu CP. *In vivo* articular cartilage deformation: noninvasive quantification of intratissue strain during joint contact in the human knee. Sci Rep 2016;6:19220.
17. Wong BL, Bae WC, Chun J, Gratz KR, Lotz M, Sah RL. Biomechanics of cartilage articulation: effects of lubrication and degeneration on shear deformation. Arthritis Rheum 2008;58:2065–74.
18. Hosseini SM, Wilson W, Ito K, van Donkelaar CC. A numerical model to study mechanically induced initiation and progression of damage in articular cartilage. Osteoarthritis Cartilage 2014;22:95–103.
19. Hayes WC, Mockros LF. Viscoelastic properties of human articular cartilage. J Appl Physiol 1971;31:562–8.
20. Zhu WB, Mow VC, Koob TJ, Eyre DR. Viscoelastic shear properties of articular cartilage and the effects of glycosidase treatments. J Orthop Res 1993;11:771–81.
21. Maier FS, Drissi H, Pierce DM. Shear deformations of human articular cartilage: certain mechanical anisotropies apparent at large but not small shear strains. J Mech Behav Biomed Mater 2017;65:53–65.
22. Below S, Arnoczky SP, Dodds J, Kooima C, Walter N. The split-line pattern of the distal femur: a consideration in the

orientation of autologous cartilage grafts. Arthroscopy 2002;18:613–7.
23. Blankevoort L, Kuiper JH, Huiskes R, Grootenboer HJ. Articular contact in a three-dimensional model of the knee. J Biomech 1991;24:1019–31.
24. Morel V, Quinn TM. Cartilage injury by ramp compression near the gel diffusion rate. J Orthop Res 2004;22:145–51.
25. Changoor A, Nelea M, Méthot S, Tran-Khanh N, Chevrier A, Restrepo A, *et al.* Structural characteristics of the collagen network in human normal, degraded and repair articular cartilages observed in polarized light and scanning electron microscopies. Osteoarthritis Cartilage 2011;19:1458–68.
26. van Wijk XMR, Vallen MJ, van de Westerlo EM, Oosterhof A, Hao W, Versteeg EM, *et al.* Extraction and structural analysis of glycosaminoglycans from formalin-fixed, paraffin-embedded tissues. Glycobiology 2012;22:1666–72.
27. Santos S, Maier F, Pierce DM. Anisotropy and inter-condyle heterogeneity of cartilage under large-strain shear. J Biomech 2017;52:74–82.
28. Pauli C, Whiteside R, Heras FL, Nesic D, Koziol J, Grogan SP, *et al.* Comparison of cartilage histopathology assessment systems on human knee joints at all stages of osteoarthritis development. Osteoarthritis Cartilage 2012;20:476–85.
29. Mow VC, Gu WY, Chen FH. Structure and function of articular cartilage and meniscus. In: Mow VC, Huiskes R, Eds. Basic Orthopaedic Biomechanics & Mechano-Biology. 3rd edn. Philadelphia: Lippincott Williams & Wilkins; 2005: 181–258.
30. Temple-Wong MM, Bae WC, Chen MQ, Bugbee WD, Amiel D, Coutts RD, *et al.* Biomechanical, structural, and biochemical indices of degenerative and osteoarthritic deterioration of adult human articular cartilage of the femoral condyle. Osteoarthritis Cartilage 2009;17:1469–76.
31. Mansour JM. Biomechanics of cartilage. In: Oatis C, Ed. Kinesiology: The Mechanics and Pathomechanics of Human Movement. Philadelphia, PA: Lippincott Williams and Wilkins; 2003:66–79.
32. Mow VC, Huiskes R. Structure and function of ligaments and tendons. In: Woo SLY, Lee TQ, Abramowitch SD, Gilbert TW, Eds. Basic Orthopaedic Biomechanics and Mechano-Biology. Philadelphia: Lippincott Williams & Wilkins; 2005:301–42.
33. Mekota AM, Vermehren M. Determination of optimal rehydration, fixation and staining methods for histological and immunohistochemical analysis of mummified soft tissues. Biotech Histochem 2005;80:7–13.
34. Hunziker EB, Lippuner K, Shintani N. How best to preserve and reveal the structural intricacies of cartilaginous tissue. Matrix Biol 2014;39:33–43.
35. Kansu L, Aydin E, Akkaya H, Avci S, Akalin N. Shrinkage of nasal mucosa and cartilage during formalin fixation. Balkan Med J 2017;34:458–63.
36. Huang CY, Stankiewicz A, Ateshian GA, Mow VC. Anisotropy, inhomogeneity, and tension-compression nonlinearity of human glenohumeral cartilage in finite deformation. J Biomech 2005;38:799–809.
37. Silverberg JL, Dillavou S, Bonassar L, Cohen I. Anatomic variation of depth-dependent mechanical properties in neonatal bovine articular cartilage. J Orthop Res 2013;31:686–91.
38. Abdel-Sayed P, Moghadam MN, Salomir R, Tchernin D, Pioletti DP. Intrinsic viscoelasticity increases temperature in knee cartilage under physiological loading. J Mech Behav Biomed Mater 2014;30:123–30.
39. Workman J, Thambyah A, Broom N. The influence of early degenerative changes on the vulnerability of articular cartilage to impact-induced injury. Clin Biomech 2017;43:40–9.
40. Nimeskern L, Utomo L, Lehtoviita I, Fessel G, Snedeker JG, van Osch GJVM, *et al.* Tissue composition regulates distinct viscoelastic responses in auricular and articular cartilage. J Biomech 2016;49:344–52.
41. June RK, Fyhrie DP. Enzymatic digestion of articular cartilage results in viscoelasticity changes that are consistent with polymer dynamics mechanisms. Biomed Eng Online 2009;8:32.
42. Griffin DJ, Vicari J, Buckley MR, Silverberg JL, Cohen I, Bonassar LJ. Effects of enzymatic treatments on the depth-dependent viscoelastic shear properties of articular cartilage. J Orthop Res 2014;32:1652–7.
43. Abdel-Sayed P, Darwiche SE, Kettenberger U, Pioletti DP. The role of energy dissipation of polymeric scaffolds in the mechanobiological modulation of chondrogenic expression. Biomaterials 2014;35:1890–7.
44. Moshtagh PR, Pouran B, van Tiel J, Rauker J, Zuiddam MR, Arbabi V, *et al.* Micro- and nano-mechanics of osteoarthritic cartilage: the effects of tonicity and disease severity. J Mech Behav Biomed Mater 2016;59:561–71.
45. Temple MM, Bae WC, Chen MQ, Lotz M, Amiel D, Coutts RD, *et al.* Age- and site-associated biomechanical weakening of human articular cartilage of the femoral condyle. Osteoarthritis Cartilage 2007;15:1042–52.
46. Buckley MR, Bonassar LJ, Cohen I. Localization of viscous behavior and shear energy dissipation in articular cartilage under dynamic shear loading. J Biomech Eng 2013;135.031002–031002–9.
47. Desrochers J, Amrein MW, Matyas JR. Viscoelasticity of the articular cartilage surface in early osteoarthritis. Osteoarthritis Cartilage 2012;20:413–21.
48. Brommer H, Laasanen MS, Brama PAJ, Weeren PRV, Helminen HJ, Jurelin JS. In situ and ex vivo evaluation of an arthroscopic indentation instrument to estimate the health status of articular cartilage in the equine metacarpophalangeal joint. Vet Surg 2006;35:259–66.
49. Kiviranta P, Lammentausta E, Töyrös J, Kiviranta I, Jurvelin JS. Indentation diagnostics of cartilage degeneration. Osteoarthritis Cartilage 2008;16:796–804.
50. Nguyen AM, Levenston ME. Comparison of osmotic swelling influences on meniscal fibrocartilage and articular cartilage tissue mechanics in compression and shear. J Orthop Res 2012;30:95–102.
51. Guermazi A, Roemer FW, Burstein D, Hayashi D. Why radiography should no longer be considered a surrogate outcome measure for longitudinal assessment of cartilage in knee osteoarthritis. Arthritis Res Ther 2011;13:247.
52. Huang C, Niethammer M, Shan L, Charles C, Zhu H. Diseased region detection of longitudinal knee MRI data. Inf Process Med Imaging 2013;23:632–43.
53. Muehleman C, Bareither D, Huch K, Cole AA, Kuettner KE. Prevalence of degenerative morphological changes in the joints of the lower extremity. Osteoarthritis Cartilage 1997;5:23–37.
54. Deneweth JM, Arruda EM, McLean SG. Hyperelastic modeling of location-dependent human distal femoral cartilage mechanics. Int J Non Lin Mech 2015;68:146–56.
55. Huang CY, Mow VC, Ateshian GA. The role of flow-independent viscoelasticity in the biphasic tensile and compressive responses of articular cartilage. J Biomech Eng 2001;123:410–7.
56. Huang CY, Soltz MA, Kopacz M, Mow VC, Ateshian GA. Experimental verification of the roles of intrinsic matrix viscoelasticity and tension-compression nonlinearity in the biphasic response of cartilage. J Biomech Eng 2003;125:84–93.